

# Thermoelectric Properties of Binary Semiconducting Intermetallic Compounds $\text{Al}_2\text{Ru}$ and $\text{Ga}_2\text{Ru}$ Synthesized by Spark Plasma Sintering Process

Yoshiki Takagiwa<sup>1</sup>, Yuka Matsubayashi<sup>1</sup>, Akitoshi Suzumura<sup>1</sup>,  
Junpei Tamura Okada<sup>2</sup> and Kaoru Kimura<sup>1</sup>

<sup>1</sup>Department of Advanced Materials Science, The University of Tokyo, Kashiwa 277-8561, Japan

<sup>2</sup>Department of Space Biology and Microgravity Sciences, Japan Aerospace Exploration Agency, Tsukuba 305-8505, Japan

The authors report the electrical and thermal transport properties of binary semiconducting intermetallic  $\text{Al}_2\text{Ru}$  and  $\text{Ga}_2\text{Ru}$  compounds from 373 to 973 K. We synthesized sintered pellets of  $\text{Al}_2\text{Ru}$  and  $\text{Ga}_2\text{Ru}$  by the spark plasma sintering (SPS) method, resulted in a removal of small amount of a secondary phase and of cracks. The maximum Seebeck coefficient of  $\text{Al}_2\text{Ru}$  and  $\text{Ga}_2\text{Ru}$  shows a large positive value of  $200\ \mu\text{V}/\text{K}$  and  $360\ \mu\text{V}/\text{K}$ , respectively. In particular, a large power factor  $\sim 2.8\ \text{mW}/\text{m}\cdot\text{K}^2$  was obtained at 773 K in  $\text{Ga}_2\text{Ru}$  compound. The dimensionless figures of merit  $ZT$  of sintered  $\text{Al}_2\text{Ru}$  and  $\text{Ga}_2\text{Ru}$  samples monotonically increase with increasing temperature and reach a maximum value of 0.20 and 0.45 at about 873 K and 773 K, respectively. [doi:10.2320/matertrans.E-M2010807]

(Received November 17, 2009; Accepted February 9, 2010; Published April 15, 2010)

**Keywords:** thermoelectric material, narrow-band-gap semiconductor, ruthenium aluminide, ruthenium gallide, spark plasma sintering

## 1. Introduction

Thermoelectric materials can be used to create devices that generate power through the direct conversion of thermal energy to electrical energy. The potential of thermoelectric materials is defined by the dimensionless figure of merit,  $ZT = S^2\sigma T/\kappa$ , where  $S$ ,  $\sigma$ ,  $\kappa$ , and  $T$  are the Seebeck coefficient, the electrical conductivity, the total thermal conductivity, and the temperature, respectively. One of the criteria for the practical application of thermoelectric materials is that  $ZT$  is desired to be above unity. To obtain a high  $ZT$  value, the Seebeck coefficient and electrical conductivity should be large while the thermal conductivity should be low. Recently, a very large  $ZT$  exceeding 2.0 has been reported in  $\text{SrTiO}_3$  for two-dimensional electron gas.<sup>1)</sup> While low-dimensional materials are likely to exhibit a high  $ZT$  value, bulk materials are also important for practical use in, for example, industrial processes.

Unconventional semiconductors such as  $\text{FeSi}$ <sup>2)</sup> have attracted attention for thermoelectric applications. While alloys composed of metallic constituents are naturally expected to be metallic, hybridization between transition metals (TM) and group III and IV elements, such as Al, Ga, and Si, leads to a band gap in the  $d$  bands near the Fermi level, as confirmed by theoretical calculations.<sup>3)</sup> A comparatively narrow band gap, a few hundred meV, near the Fermi level is expected to cause a large absolute value of the Seebeck coefficient, which is desirable to obtain a high electric power.

Takeuchi *et al.*<sup>4)</sup> reported the composition dependence of the thermoelectric properties of  $\alpha$ -AlReSi alloy system, and discussed the cause of the strong composition dependence of the thermoelectric properties in terms of their electronic structure. In this material, strong covalent bonds between Al-Al atoms and Al-TM atoms are experimentally observed by the maximum entropy method (MEM)/Rietveld analysis,<sup>5)</sup> and are attributed to the formation of the pseudogap near the Fermi level. For Al-Pd-(Mn or Re) quasicrystals, the

pseudogap is deeper than that for the approximant crystals because of a more isotropic structure. Therefore, these quasicrystals have a much higher  $ZT$  value than the approximants.<sup>6,7)</sup> Nishino *et al.*,<sup>8,9)</sup> revealed that the temperature dependence of the electrical resistivity for Heusler-type  $\text{Fe}_2\text{VAl}$  exhibited a semiconducting behavior. Recently, the electronic properties of  $\text{Fe}_2\text{VAl}_{1-x}\text{M}_x$  (M: B, In, Si) alloys have been systematically investigated by Vasundhara *et al.*<sup>10)</sup> As pointed out by Mahan and Sofo,<sup>11)</sup> a narrow peak in the density of states (DOS) at a few  $k_B T$  from the Fermi level can be beneficial for improving the thermoelectric performance. The above mentioned materials, indeed, possess relatively large Seebeck coefficients and high power factors  $S^2\sigma$ .

In this study, we focus attention on the binary semiconducting intermetallic compound  $\text{Al}_2\text{Ru}$  family because it has been investigated as a material related to the Al-TM-based quasicrystal.<sup>12,13)</sup> They possess the orthorhombic  $\text{TiSi}_2$  structure, which has the space group  $Fddd$  with 24 atoms per unit cell. Basov *et al.*<sup>14)</sup> observed that the  $\text{Al}_2\text{Ru}$  is infrared active, indicating the presence of a gap. Mandrus *et al.*<sup>15)</sup> reported the temperature dependence of the thermoelectric properties of the  $\text{Al}_2\text{Ru}$ . However, they claimed that the  $\text{Al}_2\text{Ru}$  and this class of intermetallic compounds are probably not a fruitful place ( $ZT \sim 0.07$  at 800 K)<sup>15)</sup> to search for novel thermoelectric materials because of the comparatively high thermal conductivity of about  $13\ \text{W}/\text{m}\cdot\text{K}$  at room temperature. To lower the thermal conductivity, we synthesized  $\text{Ga}_2\text{Ru}$  compound, formed by fully replacing Al with heavier Ga atoms in the  $\text{Al}_2\text{Ru}$ . The temperature dependence of the electrical conductivity under 673 K has been reported by Evers *et al.*,<sup>16)</sup> and pioneering studies on the thermoelectric properties have been reported by Amagai *et al.*<sup>17)</sup> The maximum  $ZT$  value of the hot-pressed  $\text{Ga}_2\text{Ru}$  showed 0.3 at 780 K, which was significantly smaller than that of practical thermoelectric materials. In this article, we report the thermoelectric properties of  $\text{Al}_2\text{Ru}$  and  $\text{Ga}_2\text{Ru}$  synthesized by using the spark plasma sintering (SPS) process.

## 2. Experimental Procedure

$\text{Al}_2\text{Ru}$  and  $\text{Ga}_2\text{Ru}$  mother ingots were synthesized by an arc-melting technique under a purified argon atmosphere. The samples were annealed at 1273 K for 24 h. After annealing, the samples were quenched in water. However, there are some cracks and pores in the arc-melted and annealed sample, which should decrease the electrical conductivity. To improve the microstructure, we synthesized a sintered sample by the SPS method. As for the  $\text{Al}_2\text{Ru}$ , Al and Ru powder was placed in a carbon die with a diameter of 10 mm for the SPS processing on SPS SYNTEX INC. (DR. SINTER. LAB., SPS-515S). The temperature of the specimen was increased from ambient temperature to 873 K in 5 min, and from 873 K to the consolidating temperature of 1223 K in 5 min, and then the consolidating temperature was held for 30 min. A pressure of 4.5 kN was applied during the heating process. After the SPS treatment, the specimen was cooled to ambient temperature under an argon atmosphere applying pressure of 2.5 kN. The sintered sample was annealed at 1023 K for 24 h and 1223 K for 24 h. To obtain a single phase of the  $\text{Al}_2\text{Ru}$ , we reduced about 4 mass% of Ru powder from stoichiometric composition. As for the  $\text{Ga}_2\text{Ru}$ , the arc-melted and annealed sample was crushed to an average particle size of below 20  $\mu\text{m}$ . The powder was placed in a carbon die with a diameter of 10 mm. The temperature of the specimen was increased from ambient temperature to 873 K in 5 min, and from 873 K to the consolidating temperature of 1223 K in 5 min, and then the consolidating temperature was held for 10 min. A pressure of 3.3 kN was applied during the heating process. After the SPS treatment, the specimen was cooled to ambient temperature under an argon atmosphere applying pressure of 2.5 kN.

The characterization of the samples was performed by powder X-ray diffraction (XRD) measurements with Cu  $K\alpha$  radiation. The local compositions were examined by electron probe microanalysis (EPMA). The electrical conductivity and Seebeck coefficient were measured in a helium atmosphere at temperatures between 373 and 973 K by the four-probe method and the steady-state temperature gradient method, respectively. The thermal conductivity was obtained by measuring the density, specific heat and thermal diffusivity from 300 to 973 K by the laser flash method. Hall coefficient measurements were performed for the sintered  $\text{Ga}_2\text{Ru}$  at ambient temperature. The Debye temperatures were calculated from the transverse and longitudinal sound velocities measured by the ultrasonic pulse echo method (Nihon Matech Corp., Echometer 1062).

## 3. Sample Characterization

Figure 1 shows experimental and calculated XRD patterns of the  $\text{Al}_2\text{Ru}$ . In the arc-melted and annealed (arc-melted) sample (a), there exist a secondary phase of  $\text{AlRu}$ . On the other hand, we could obtain a pattern of single phase for  $\text{Al}_2\text{Ru}$  in sintered and annealed (sintered) sample (b), which agrees well with the calculated pattern (c). Figure 2 shows experimental and calculated XRD patterns of the  $\text{Ga}_2\text{Ru}$ . Very weak peaks of a secondary phase of  $\text{Ga}_3\text{Ru}$  were observed in the arc-melted and annealed (arc-melted) sample

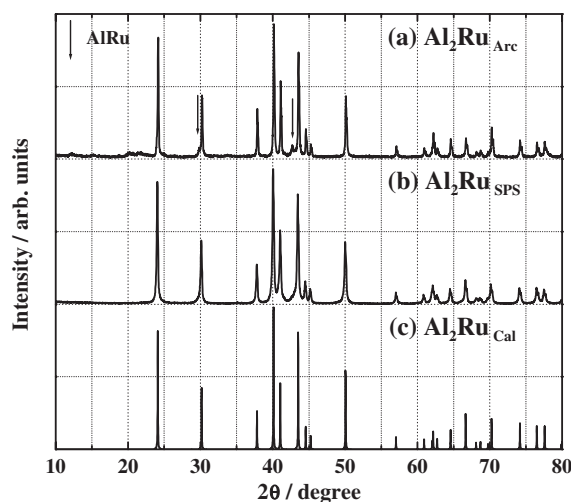


Fig. 1 X-ray diffraction patterns of (a) arc-melted and annealed (arc-melted), (b) sintered and annealed (sintered)  $\text{Al}_2\text{Ru}$  samples. Pattern (c) is a calculated pattern. Arrows show the peak of a secondary phase of  $\text{AlRu}$ .

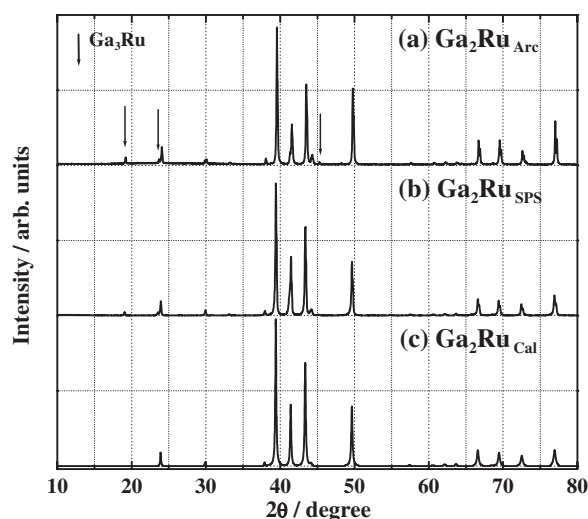


Fig. 2 X-ray diffraction patterns of (a) arc-melted and annealed (arc-melted), (b) arc-melted, annealed and sintered (sintered)  $\text{Ga}_2\text{Ru}$  samples. Pattern (c) is a calculated pattern. Arrows show the peak of a secondary phase of  $\text{Ga}_3\text{Ru}$ .

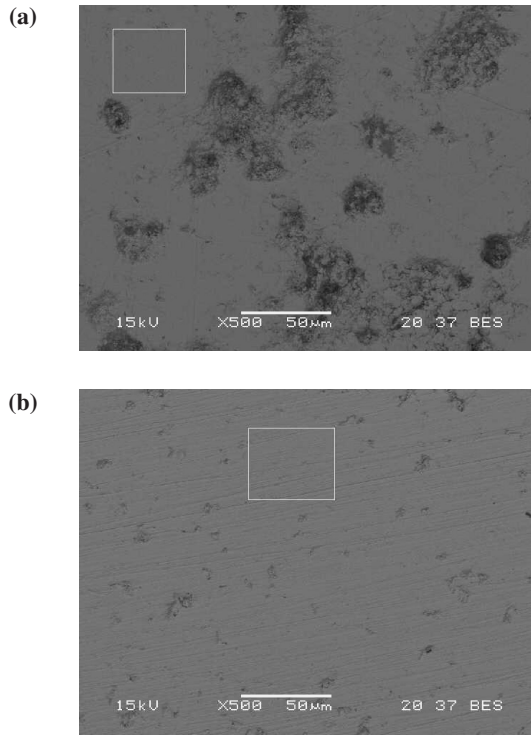
Table 1 Lattice parameters of  $\text{Al}_2\text{Ru}$  and  $\text{Ga}_2\text{Ru}$  determined by the Rietveld analysis.

$\text{Al}_2\text{Ru}$	$R_{\text{wp}} = 7.92\%$ , $R_1 = 6.47\%$		
<i>Fddd</i>	<i>a</i> (nm)	<i>b</i> (nm)	<i>c</i> (nm)
No. 70	0.80106	0.47156	0.87879
$\text{Ga}_2\text{Ru}$	$R_{\text{wp}} = 2.77\%$ , $R_1 = 2.06\%$		
<i>Fddd</i>	<i>a</i> (nm)	<i>b</i> (nm)	<i>c</i> (nm)
No. 70	0.81903	0.47466	0.87119

(a). On the other hand, the amount of the secondary phase of  $\text{Ga}_3\text{Ru}$  significantly decreases in the arc-melted, annealed and sintered (sintered) sample (b). A measured XRD pattern agrees well with the calculated pattern (c). Table 1 lists the lattice constants of the  $\text{Al}_2\text{Ru}$  and  $\text{Ga}_2\text{Ru}$  determined by the Rietveld analysis. The densities are 6.50 and 9.61  $\text{g}/\text{cm}^3$  for the  $\text{Al}_2\text{Ru}$  and  $\text{Ga}_2\text{Ru}$ , respectively. The relative densities of

Table 2 Averaged microprobe compositions of sintered  $\text{Al}_2\text{Ru}$  and  $\text{Ga}_2\text{Ru}$  samples.

sample	nominal composition	averaged microprobe composition
$\text{Al}_2\text{Ru}$	$\text{Al}_{68}\text{Ru}_{32}$	$\text{Al}_{64.8}\text{Ru}_{35.2}$
$\text{Ga}_2\text{Ru}$	$\text{Ga}_{67}\text{Ru}_{33}$	$\text{Ga}_{68.4}\text{Ru}_{31.6}$

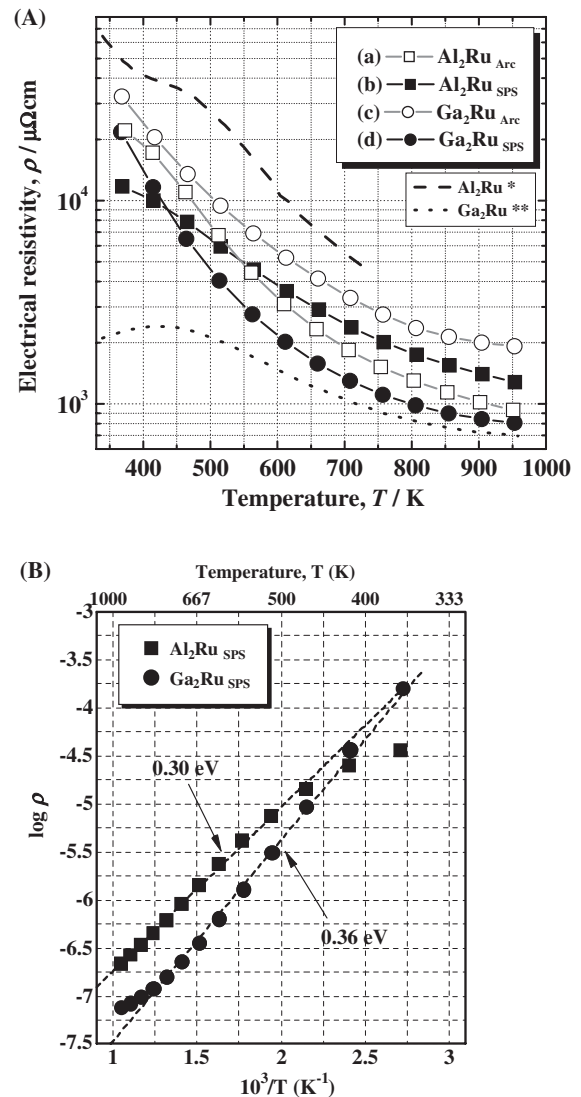
Fig. 3 Back scattered electron images of sintered (a)  $\text{Al}_2\text{Ru}$  and (b)  $\text{Ga}_2\text{Ru}$  samples. White box shows one of the areas for composition analysis by EPMA.

the sintered  $\text{Al}_2\text{Ru}$  and  $\text{Ga}_2\text{Ru}$  are 95%. The (SPS) sintered bulk density ( $6.16 \text{ g/cm}^3$ ) of the  $\text{Al}_2\text{Ru}$  is significantly larger than that ( $5.765 \text{ g/cm}^3$ )<sup>15)</sup> of hot-pressed sample by Mandrus *et al.* This is due to a high relative density and slightly Ru-rich sample (as listed in Table 2) for the (SPS) sintered sample.

Figure 3 shows back scattered electron images (BEI) of the sintered  $\text{Al}_2\text{Ru}$  and  $\text{Ga}_2\text{Ru}$  samples. While there are some pores (black area) in the  $\text{Al}_2\text{Ru}$ , few pores are observed in the  $\text{Ga}_2\text{Ru}$ . There are no cracks both in the sintered  $\text{Al}_2\text{Ru}$  and  $\text{Ga}_2\text{Ru}$  samples. We cannot observe the secondary phases of  $\text{AlRu}$  and  $\text{Ga}_3\text{Ru}$  in the sintered  $\text{Al}_2\text{Ru}$  and  $\text{Ga}_2\text{Ru}$ , respectively. Table 2 lists the nominal compositions and averaged microprobe compositions obtained by using EPMA.

#### 4. Thermoelectric Properties

The electrical resistivity  $\rho$  of the  $\text{Al}_2\text{Ru}$  and  $\text{Ga}_2\text{Ru}$  from 373 to 973 K is plotted in Fig. 4(A). The previous reported data of hot-pressed  $\text{Al}_2\text{Ru}$ <sup>15)</sup> and  $\text{Ga}_2\text{Ru}$ <sup>17)</sup> are also plotted.  $\rho$  exhibits a semiconducting behavior both in the  $\text{Al}_2\text{Ru}$  and  $\text{Ga}_2\text{Ru}$ . As for the  $\text{Al}_2\text{Ru}$ ,  $\rho_{373\text{K}}$  of the sintered sample is significantly lower than that of the arc-melted sample or hot-pressed sample.<sup>15)</sup> This is due to the fact that the (SPS)

Fig. 4 (A) Electrical resistivity as a function of temperature and (B) Natural logarithm of electrical resistivity as a function of inverse temperature, of (a) arc-melted, (b) sintered  $\text{Al}_2\text{Ru}$  samples, and (c) arc-melted, (d) sintered  $\text{Ga}_2\text{Ru}$  samples. The previous reported data of  $\text{Al}_2\text{Ru}$  and  $\text{Ga}_2\text{Ru}$  are plotted in dashed and dotted lines. \*15), \*\*17)

sintered sample does not contain any cracks. However, the trend of  $\rho$  was changed above 573 K: the arc-melted sample shows lower electrical resistivity than the sintered sample, which comes from the existence of metallic secondary phase of  $\text{AlRu}$  as confirmed by XRD. As for the  $\text{Ga}_2\text{Ru}$ ,  $\rho$  of the sintered sample is markedly lower than that of the arc-melted sample in the overall temperatures, but is higher than the hot-pressed sample.<sup>17)</sup> The former trend is because the arc-melted sample contains a lot of cracks and a nonmetallic secondary phase of  $\text{Ga}_3\text{Ru}$ . Indeed,  $\text{Ga}_3\text{Ru}$  exhibits relatively higher electrical resistivity ( $\sim 10^2 \text{ m}\Omega\text{cm}$ ),<sup>18)</sup> which is one-order higher than that of the  $\text{Ga}_2\text{Ru}$ . We cannot discuss the latter trend at this stage because the bulk density or microprobe composition of hot-pressed  $\text{Ga}_2\text{Ru}$  is not described in the Ref. 17).

Above 500 K,  $\rho$  obeys the Arrhenius law  $\rho(T) = \rho_0 e^{\Delta/k_B T}$ , as shown in Fig. 4(B). As there exist a secondary phase both in the arc-melted samples of the  $\text{Al}_2\text{Ru}$  and  $\text{Ga}_2\text{Ru}$ , we compare the estimated values of activation energy  $\Delta$  of

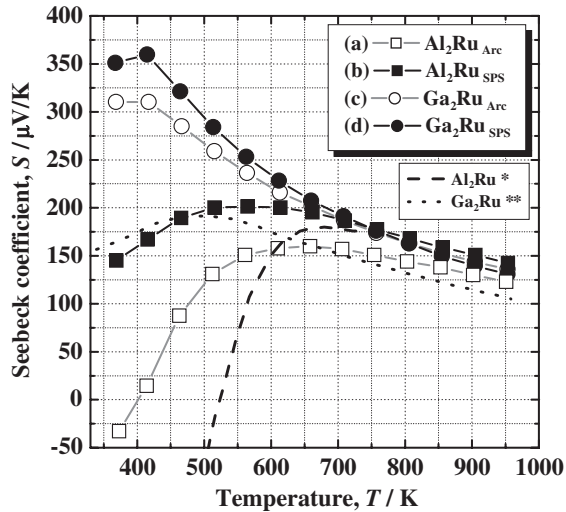


Fig. 5 Seebeck coefficient  $S$  as a function of temperature of (a) arc-melted, (b) sintered Al<sub>2</sub>Ru samples, and (c) arc-melted, (d) sintered Ga<sub>2</sub>Ru samples. The previous reported data of Al<sub>2</sub>Ru and Ga<sub>2</sub>Ru are plotted in dashed and dotted lines. \*<sup>15</sup>, \*\*<sup>17</sup>)

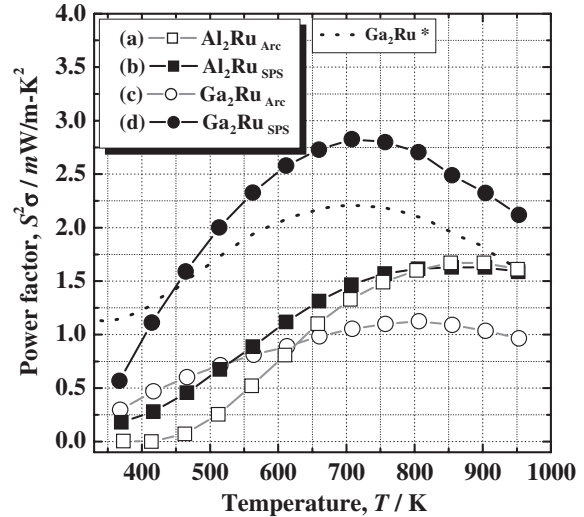


Fig. 6 Power factor  $S^2\sigma$  as a function of temperature of (a) arc-melted, (b) sintered Al<sub>2</sub>Ru samples, and (c) arc-melted, (d) sintered Ga<sub>2</sub>Ru samples. The previous reported data of Ga<sub>2</sub>Ru is plotted in dotted line. \*<sup>17</sup>)

the sintered Al<sub>2</sub>Ru and Ga<sub>2</sub>Ru: the values are 0.15 and 0.18 eV, respectively. This yields  $E_g = 2\Delta \sim 0.30$  eV for the band gap of the Al<sub>2</sub>Ru, which is comparable with the value of 0.36 eV for the Ga<sub>2</sub>Ru. It should be mentioned here that the Al<sub>2</sub>Ru and Ga<sub>2</sub>Ru compounds possess indirect gap about 0.3 eV by using LMTO-ASA calculations<sup>19)</sup> and our calculation by WIEN2k (not shown). This indirect gap near the band-edge is suitable for high performance of thermoelectric materials.<sup>20,21)</sup>

The Seebeck coefficient  $S$  of the Al<sub>2</sub>Ru and Ga<sub>2</sub>Ru from 373 to 973 K is plotted in Fig. 5. A large positive  $S$  was observed in the overall temperatures except for the arc-melted Al<sub>2</sub>Ru. The maximum  $S$  value of the Al<sub>2</sub>Ru and Ga<sub>2</sub>Ru are  $\sim 200$  and  $\sim 360$   $\mu\text{V}/\text{K}$ , respectively. As  $S$  of Ga<sub>3</sub>Ru below 500 K exhibits negative value,<sup>18)</sup> therefore, it is reasonable to state that the difference in  $S$  between arc-melted and sintered Ga<sub>2</sub>Ru samples is caused by the secondary phase of Ga<sub>3</sub>Ru. On the other hand, comparative large difference in  $S$  between the arc-melted and sintered Al<sub>2</sub>Ru samples will be caused by a metallic secondary phase of AlRu. From the shape of the density of states (DOS) of the Al<sub>2</sub>Ru and Ga<sub>2</sub>Ru,<sup>19)</sup> it is easily expected that  $S$  and  $\sigma$  is strongly affected by the position of the Fermi level. Therefore, the discrepancy in  $S$  between our results and the previous data<sup>15,17)</sup> will be attributed to the sample's compositions. Because the room-temperature Hall coefficient is *positive* for the Ga<sub>2</sub>Ru, it is obvious that holes dominantly contribute to the conduction. The carrier density and mobility of the Ga<sub>2</sub>Ru are  $1.13 \times 10^{18} \text{ cm}^{-3}$  and  $129 \text{ cm}^2/\text{V}\cdot\text{s}$  at 300 K, respectively. This result is consistent with the band-structure calculations, which predict that the Al<sub>2</sub>Ru and Ga<sub>2</sub>Ru compounds are narrow-band-gap semiconductors with a light hole pocket and heavier electron pockets.<sup>19,22,23)</sup>

Figure 6 shows the power factor  $S^2\sigma$  of the Al<sub>2</sub>Ru and Ga<sub>2</sub>Ru as a function of temperature. A large positive  $S^2\sigma$  ( $2.8 \text{ mW}/\text{m}\cdot\text{K}^2$  around 700 K) was observed in the sintered Ga<sub>2</sub>Ru, which is significantly higher than the previous reported data ( $\sim 2.2 \text{ mW}/\text{m}\cdot\text{K}^2$ ) by Amagai *et al.*<sup>17)</sup> This

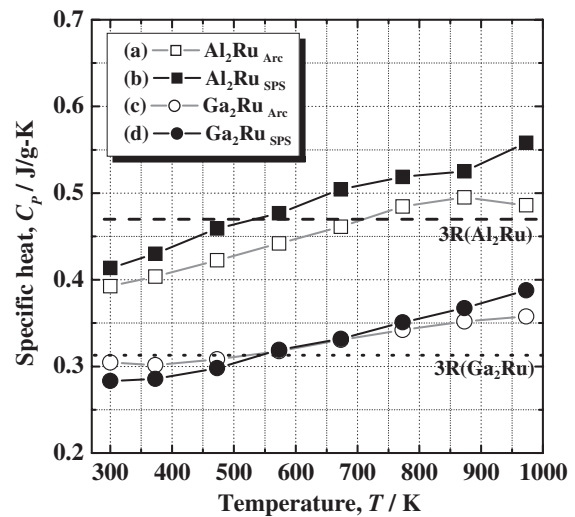


Fig. 7 Specific heat  $C_p$  as a function of temperature of (a) arc-melted, (b) sintered Al<sub>2</sub>Ru samples, and (c) arc-melted, (d) sintered Ga<sub>2</sub>Ru samples. The dashed (Al<sub>2</sub>Ru) and dotted (Ga<sub>2</sub>Ru) lines indicate the Dulong and Petit limit.

$S^2\sigma_{\text{max}}$  value is comparable with the practical thermoelectric materials. On the other hand,  $S^2\sigma$  value of the sintered Al<sub>2</sub>Ru shows  $1.6 \text{ mW}/\text{m}\cdot\text{K}^2$  around 800 K whose value is slightly higher than that of the result by Muta *et al.*<sup>24)</sup> The thermoelectric performance dramatically increases more than one and a half times by replacing Al with Ga atoms for sintered single phase samples. The origin of higher  $\sigma$  of the Ga<sub>2</sub>Ru than that of the Al<sub>2</sub>Ru is caused by fewer pores. A comparative low  $S^2\sigma$  of the arc-melted and annealed Ga<sub>2</sub>Ru ( $1.1 \text{ mW}/\text{m}\cdot\text{K}^2$ ) is originated from the high electrical resistivity, brought by an extrinsic origin such as cracks.

We measured the specific heat  $C_p$  of the Al<sub>2</sub>Ru and Ga<sub>2</sub>Ru by using the laser flash method. Figure 7 represents  $C_p$  as a function of temperature from 300 to 973 K. Because an error of  $C_p$  is considered to be about  $\pm 10\%$ , there is no significant difference in  $C_p$  between the arc-melted and sintered samples

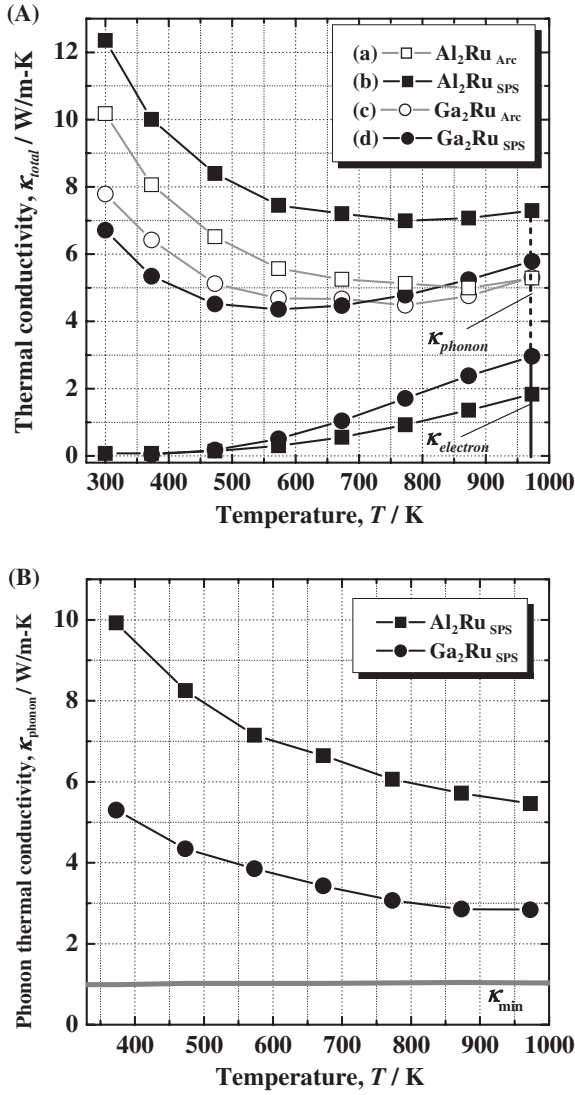


Fig. 8 (A) Total thermal conductivity  $\kappa_{total}$  and electron thermal conductivity  $\kappa_{electron}$ , and (B) lattice thermal conductivity  $\kappa_{phonon}$ , as a function of temperature of (a) arc-melted, (b) sintered  $\text{Al}_2\text{Ru}$  samples, and (c) arc-melted, (d) sintered  $\text{Ga}_2\text{Ru}$  samples. The minimum thermal conductivity  $\kappa_{min}$  is also presented in (B).

of the  $\text{Al}_2\text{Ru}$  and  $\text{Ga}_2\text{Ru}$ .  $C_p$  of the  $\text{Al}_2\text{Ru}$  and  $\text{Ga}_2\text{Ru}$  exhibit about 0.4 and 0.3 J/g-K at 300 K, respectively. The difference in  $C_p$  can be explained by the difference in the mass between the  $\text{Al}_2\text{Ru}$  (6.16 g/cm<sup>3</sup>) and  $\text{Ga}_2\text{Ru}$  (9.02 g/cm<sup>3</sup>). We readily see that the curves approach asymptotically the value of 3R, that is, the Dulong and Petit limit. As the temperature is further increased, they cross this limit and continue to increase. This phenomenon is also observed in pure metals such as aluminum and copper.

Figure 8(A) shows the temperature dependence of the total thermal conductivity  $\kappa_{total}$ , together with the electronic contribution  $\kappa_{electron}$  estimated using the well-known Wiedemann-Franz law expressed by  $\kappa_{electron} = L_0\sigma T$ , where  $L_0$  is the Lorentz number. We assumed  $L_0$  to be  $2.45 \times 10^{-8} \text{ V}^2/\text{K}^2$ .  $\kappa_{total}$  of the  $\text{Ga}_2\text{Ru}$  is 7–8 W/m-K at 300 K, which is beneficially lower than that (10–12 W/m-K) of the  $\text{Al}_2\text{Ru}$ . The room temperature magnitude of  $\kappa_{total}$  of the sintered  $\text{Ga}_2\text{Ru}$  is  $\sim 7$  W/m-K that is consistent with the previous result of hot-pressed sample.<sup>17)</sup>  $\kappa_{total}$  first decreases

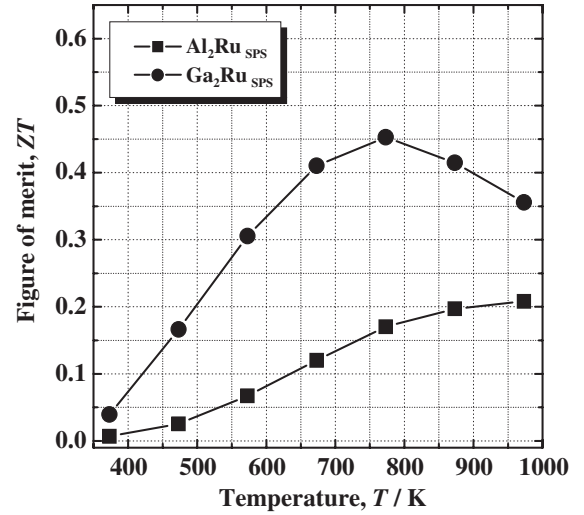


Fig. 9 Dimensionless figure of merit  $ZT$  as a function of temperature of sintered  $\text{Al}_2\text{Ru}$  and  $\text{Ga}_2\text{Ru}$  samples.

with increasing temperature up to 600 K, and then slightly increases with increasing temperature; this is mainly brought by the increase in the electronic contribution. It should be mentioned here that the samples for the thermal conductivity measurement were different from the samples for the electrical resistivity and Seebeck coefficient measurement, which means that, for the arc-melted samples, the situation of cracks and second phases, and their effects to the physical properties are different in the two samples. This causes that  $\kappa_{electron}$  of the arc-melted samples cannot be evaluated accurately. Thus, we estimate and compare the lattice thermal conductivity  $\kappa_{phonon}$  ( $= \kappa_{total} - \kappa_{electron}$ ) for only the sintered samples as shown in Fig. 8(B). As for the sintered samples, it was observed that the  $\text{Ga}_2\text{Ru}$  with heavier atomic weight have the lower  $\kappa_{phonon}$ . This can be understood by the difference in the Debye temperature  $\theta_D$ , 520 K and 450 K, of the sintered  $\text{Al}_2\text{Ru}$  and  $\text{Ga}_2\text{Ru}$  samples, respectively. We calculated the minimum lattice thermal conductivity  $\kappa_{min}$  for the  $\text{Ga}_2\text{Ru}$  using the model proposed by Cahill *et al.*<sup>25)</sup> The calculated  $\kappa_{min}$  is about 1.0 W/m-K above 373 K as plotted in Fig. 8(B), which is about one-third of the sintered  $\text{Ga}_2\text{Ru}$  sample.

## 5. Estimation of Figure of Merit

Finally, we present the dimensionless figure of merit  $ZT$  of the  $\text{Al}_2\text{Ru}$  and  $\text{Ga}_2\text{Ru}$  from 373 to 973 K in Fig. 9. The maximum  $ZT$  value  $ZT_{max}$  of the sintered  $\text{Al}_2\text{Ru}$  exhibits 0.20 above 900 K, which is significantly higher than the previous report (0.07 at 800 K).<sup>15)</sup> This is mainly brought by the decrease in the electrical resistivity because of removing cracks. On the other hand, the sintered  $\text{Ga}_2\text{Ru}$  exhibits  $ZT_{max} = 0.45$  at 773 K, which is higher than the previous report (0.3 at 780 K)<sup>17)</sup> because of better microstructure and is over twice higher than that of the sintered  $\text{Al}_2\text{Ru}$  measured in this study because of heavier mass of Ga than that of Al and the better microstructure. The *potential*  $ZT_{max}$  of the  $\text{Ga}_2\text{Ru}$  compound is  $\sim 0.74$ , as estimated using the *ideal* minimum thermal conductivity ( $= \kappa_{min} + \kappa_{electron}$ ). This result indicates that the  $\text{Ga}_2\text{Ru}$  compound is a potential candidate for a novel

thermoelectric material. Substitution of multiple elements with different masses will reduce  $\kappa_{\text{phonon}}$  via induced mass fluctuations and strain field effects.<sup>26,27)</sup> Furthermore, the power factor will increase to optimize the electronic structure via hole-doped substitutions.

## 6. Conclusions

In this study, the temperature dependence of the thermoelectric properties and the dimensionless figure of merit  $ZT$  of binary semiconducting intermetallic Al<sub>2</sub>Ru and Ga<sub>2</sub>Ru compounds were investigated. We successfully synthesized the single-phase of the Al<sub>2</sub>Ru and Ga<sub>2</sub>Ru synthesized by using the SPS process. In particular, the SPS process is more favorable than the arc-melted and annealed process because the small amounts of secondary phase and a lot of cracks can be removed. We beneficially reduced the thermal conductivity by fully replacing Ga for Al atoms in the Al<sub>2</sub>Ru. Also a large value ( $\sim 2.8 \text{ mW/m-K}^2$ ) of  $S^2\sigma$  was obtained in the sintered Ga<sub>2</sub>Ru.  $ZT$  increases with increasing temperature and reaches a maximum value of 0.45 at about 773 K. The potential  $ZT_{\text{max}}$  is about 0.74, as estimated using the ideal minimum thermal conductivity, indicating that the Ga<sub>2</sub>Ru compound is a potential candidate for a novel thermoelectric material. Substitution of multiple elements with different masses will reduce the phonon thermal conductivity and the power factor will increase to optimize the electronic structure, which can obtain a higher  $ZT$  value.

## Acknowledgments

This work is partly supported by KAKENHI No. 21860021, 19051005 and 19360286 from JSPS and the Ministry of Education, Culture, Sports, Science and Technology of Japan. One of the authors (Y. T.) acknowledges the support for this work provided by Research Fellowship of the Japan Society for the Promotion of Science (JSPS) for Young Scientists.

## REFERENCES

- 1) H. Ohta, S. Kim, Y. Mune, T. Mizoguchi, K. Nomura, S. Ohta, T. Nomura, Y. Nakanishi, Y. Ikuhara, M. Hirano, H. Hosono and K.

- Koumoto: *Nature Mater.* **6** (2007) 129–134.
- 2) Z. Schlesinger, Z. Fisk, H.-T. Zhang, M. B. Maple, J. F. DiTusa and G. Aeppli: *Phys. Rev. Lett.* **71** (1993) 1748–1751.
- 3) M. Weinert and R. E. Watson: *Phys. Rev. B* **58** (1998) 9732–9740.
- 4) T. Takeuchi, T. Otagiri, H. Sakagami, T. Kondo, U. Mizutani and H. Sato: *Phys. Rev. B* **70** (2004) 144202-1-7.
- 5) K. Kirihara, T. Nagata, K. Kimura, K. Kato, M. Takata, E. Nishibori and M. Sakata: *Phys. Rev. B* **68** (2003) 014205-1-12.
- 6) J. T. Okada, T. Hamamatsu, S. Hosoi, T. Nagata, K. Kimura and K. Kirihara: *J. Appl. Phys.* **101** (2007) 103702-1-4.
- 7) Y. Takagiwa, T. Kamimura, S. Hosoi, J. T. Okada and K. Kimura: *J. Appl. Phys.* **104** (2008) 073721-1-4.
- 8) Y. Nishino, H. Kato, M. Kato and U. Mizutani: *Phys. Rev. B* **63** (2001) 233303-1-4.
- 9) Y. Nishino, H. Sumi and U. Mizutani: *Phys. Rev. B* **71** (2005) 094425-1-8.
- 10) M. Vasundhara, V. Srinivas and V. V. Rao: *Phys. Rev. B* **77** (2008) 2244151-8.
- 11) G. D. Mahan and J. O. Sofo: *Proc. Natl. Acad. Sci. U.S.A.* **93** (1996) 7436.
- 12) F. S. Pierce, S. J. Poon and B. D. Biggs: *Phys. Rev. Lett.* **70** (1993) 3919–3922.
- 13) M. Krajci and J. Hafner: *J. Phys.: Condens. Matter* **14** (2002) 5755–5783.
- 14) D. N. Basov, F. S. Pierce, P. Volkov, S. J. Poon and T. Timusk: *Phys. Rev. Lett.* **73** (1994) 1865–1868.
- 15) D. Mandrus, V. Keppens, B. C. Sales and J. L. Sarrao: *Phys. Rev. B* **58** (1998) 3712–3716.
- 16) J. Evers, G. Oehlinger and H. Meyer: *Mat. Res. Bull.* **19** (1984) 1177–1180.
- 17) Y. Amagai, A. Yamamoto, C.-H. Lee, H. Ohara, K. Ueno, T. Iida and Y. Takanashi: *Papers of technical meeting on frontier technology and engineering*, (IEE Japan, vol. FTE-05, 2005) pp. 41–46.
- 18) Y. Amagai, A. Yamamoto, T. Iida and Y. Takanashi: *J. Appl. Phys.* **96** (2004) 5644–5648.
- 19) D. N. Manh, G. Trambly de Laissardiere, J. P. Julien, D. Mayou and F. Cyrot-Lackmann: *Solid State Commun.* **82** (1992) 329–334.
- 20) J. S. Tse and D. D. Klug: *Thermoelectrics Handbook Macro to Nano*, ed. by D. M. Rowe, (Taylor & Francis, Boca Raton, 2006) Chap. 8-1-27.
- 21) T. Takeuchi: *Mater. Trans.* **50** (2009) 2359–2365.
- 22) S. E. Burkov and S. N. Rashkeev: *Solid State Commun.* **92** (1994) 525–529.
- 23) M. Springborg and R. Fischer: *J. Phys.: Condens. Matter* **10** (1998) 701–716.
- 24) H. Muta *et al.*, private communication.
- 25) D. G. Cahill, S. K. Watson and R. O. Pohl: *Phys. Rev. B* **46** (1992) 6131–6140.
- 26) Q. Shen, L. Chen, T. Goto, T. Hirai, J. Yang, G. P. Meisner and C. Uher: *Appl. Phys. Lett.* **79** (2001) 4165–4167.
- 27) J. Yang, G. P. Meisner and L. Chen: *Appl. Phys. Lett.* **85** (2004) 1140–1142.